



Entamoeba gingivalis Exerts Severe Pathogenic Effects on the Oral Mucosa

X. Bao¹ , J. Weiner^{3rd2}, O. Meckes³, H. Dommisch¹ , and A.S. Schaefer¹

Journal of Dental Research
2021, Vol. 100(7) 771–776
© International & American Associations
for Dental Research 2021



Article reuse guidelines:
sagepub.com/journals-permissions
DOI: 10.1177/00220345211004498
journals.sagepub.com/home/jdr

Abstract

The protozoan *Entamoeba gingivalis* colonizes the healthy oral mucosa with a prevalence of 15%. Colonization can be asymptomatic, and it is considered not pathogenic. However, it is able to invade lacerated oral mucosa, where it ingests fragments of live cells, suggesting pathogenic potential. Here, we characterized the transcriptomes of gingival cells after infection with *E. gingivalis* using RNA sequencing and observed pathogen interaction with the epithelial monolayer barrier by scanning electron microscopy. In epithelial and fibroblast cells, strongest differential expression showed gene set “chemokines and inflammatory molecules in myeloid cells” (area under the curve [AUC] = 0.9, effect size 5.15, adjusted $P = 3.1 \times 10^{-19}$) and “cell cycle and growth arrest” (AUC = 0.91, effect size = 4.56, adjusted $P = 4.8 \times 10^{-9}$), respectively. The most upregulated genes were *TNF* (fold change 430) and *IL8* (fold change 359) in epithelial cells and *ZN331* (fold change 18) in fibroblasts. We showed that *E. gingivalis* killed live epithelial cells by trogocytosis, demonstrating strong pathogenic potential.

Keywords: sequence analysis, RNA, oral mucosa, tissue destruction, inflammation, microscopy

Introduction

The eukaryotic protozoan *Entamoeba gingivalis* colonizes the healthy oral cavity with a prevalence of ~15%, whereas inflamed periodontal pockets of periodontitis patients are infected with a frequency of 70% to 80% (Trim et al. 2011; Bonner et al. 2014; Bao et al. 2020). Although here, *E. gingivalis* contributes the second most abundant ribosomal RNA (rRNA) after human rRNA (Deng et al. 2017), the established paradigm has been that it does not cause or contribute to periodontal tissue destruction and inflammation. However, cell ingestion by this amoeba has been highlighted before (Lyons 1989; Bonner et al. 2014), and the status of *E. gingivalis* as a potential pathogen contributing to periodontitis is being discussed (Bonner et al. 2018). Recently, in an in vitro infection model of lacerated live ex vivo biopsies of the oral mucosa, we showed that *E. gingivalis* invades the oral mucosa, where it moves and ingests fragments of live host cells (Bao et al. 2020). Here, *E. gingivalis* formed a tube that protruded from the main body and penetrated the host cell membrane. Fragments of the inside of the host cells were ingested through the channel of this tube, a process that resembled a mechanism termed trogocytosis and was also observed for *E. gingivalis*-infected leukocytes from plaque of the periodontal pocket (Bonner et al. 2018). Trogocytosis is different from phagocytosis, in which a predatory organism uses its plasma membrane to engulf the entire food source for ingestion and was first described for the related colonic protozoan *Entamoeba histolytica* (Ralston et al. 2014). Trogocytosis expands the current model that pathogenic *Entamoeba* species would use secreted

toxic effectors to overcome the epithelial barrier and to kill cells prior to ingestion (Ralston and Petri 2011). Theoretically, trogocytosis would enable *E. gingivalis* to overcome the healthy and intact gingival epithelial barrier that is formed by the monolayer of tightly linked epithelial cells and allow subsequent invasion into the oral mucosa. However, this has not yet been shown. To get a detailed picture of the molecular effects of direct contact of *E. gingivalis* to gingival cells, we characterized the expression profiles of gingival epithelial and fibroblast cells following direct cell contact to *E. gingivalis* to specify its pathogenic potential. The second aim was to observe live host–parasite interactions to understand how this protozoon would induce human cell killing to overcome the epithelial cell monolayer barrier.

¹Charité–University Medicine Berlin, Corporate Member of Freie Universität Berlin, Humboldt-Universität zu Berlin, and Berlin Institute of Health, Institute for Dental and Craniofacial Sciences, Department of Periodontology, Oral Medicine and Oral Surgery, Berlin, Germany

²Core Unit Bioinformatics, Berlin Institute of Health, Berlin, Germany

³Eye of Science, Nicole Ottawa & Oliver Meckes GbR, Reutlingen, Germany

A supplemental appendix to this article is available online.

Corresponding Author:

A. Schaefer, Department of Periodontology, Oral Medicine and Oral Surgery, Institute for Dental and Craniofacial Sciences, Charité–Universitätsmedizin Berlin, Aßmannshauer Straße 4-6, Berlin, 14197, Germany.

Email: arne.schaefer@charite.de

Materials and Methods

E. gingivalis Culture

Subgingival plaque samples were collected with sterile curettes from inflamed periodontal pockets of patients who were diagnosed and treated for periodontitis in the Department of Periodontology at the Charité—University Medicine, Berlin. The subgingival plaque samples were transferred to TYGM-9 medium and cultured under anaerobic conditions in petri dishes at 35°C. A subsample of the plaque was placed into 200 μ L lysis buffer (50 mM Tris-HCL [pH 8.0], 10 mM EDTA, 2% sodium dodecyl sulfate [SDS]) for DNA extraction and subsequent detection of *E. gingivalis* by polymerase chain reaction (PCR). The presence of *E. gingivalis* in the growth medium was visually examined on a microscope after 5 d.

PCR Test for *E. gingivalis*

DNA was isolated directly from growth medium and plaque dissolved in lysis buffer using phenol-chloroform extraction (Rosenbaum et al. 2019). DNA was amplified by PCR using the *E. gingivalis* specific primers (forward: AGGAATGAA CGGAACGTACA; reverse: CCATTCCTTCTTCTATTGT TTCAC) (Bonner et al. 2014) with the following settings: 55°C annealing temperature, 30-s annealing time, 1-min elongation time, and 30 cycles.

Human Cell Culture

Immortalized human gingival epithelial cells (OKG4, purchased from Applied Biological Materials [ABM]) were cultured in DermaLife K serum-free growth medium (Lifeline Cell Technology) supplemented with 1% penicillin-streptomycin. Cells were seeded at 180,000 cells per 6-well plate (TPP Techno Plastic Products) before *E. gingivalis* infection and cultured for 2 d to reach around 80% confluence.

Infection of Human Cells with *E. gingivalis*

For the infection experiments, petri dishes containing the amoebic cultures were placed on ice for 8 min to detach amoebae from the bottom. Subsequently, the cultures were collected and transferred to sterile 2-mL Eppendorf tubes and centrifuged for 10 min at 275 *g*. The supernatant was discarded and the remaining pellet was washed with 1 mL sterile 1 \times phosphate-buffered saline (PBS) by gentle pipetting. The washing was repeated 4 times to reduce bacterial contamination from the culture, and after the last washing step, the *E. gingivalis* pellets were pooled. For RNA sequencing (RNA-Seq) experiments, after the last washing step, 10 μ L PBS containing pooled *E. gingivalis* at a multiplicity of infection (MOI) of 0.2 was added to human primary gingival epithelial cells (pGECs) and primary fibroblasts (pGFs) cultured in 6-well plates (TPP Techno Plastic Products) and cocultured for 2 h. To generate the mock infection medium, we used 10 μ L of the supernatant

of the last washing step. For the raster electron microscopy, *E. gingivalis* was washed and pooled as described above. Immortalized gingival epithelial cells (OKG4/bmi1/TERT) (Dickson et al. 2000) were grown on coverslips in 24-well plates to ~80% confluence and infected as described above. Growth medium was carefully removed, and 500 μ L 2.5% paraformaldehyde was added and incubated for 1 h at room temperature. Subsequently, 2 mL pure water was added to dilute the fixation solution to 0.5%. The samples were kept in a 24-well plate and sealed with paraffin film.

RNA-Seq

Total RNA was extracted from the cells using the RNeasy Mini Kit (Qiagen) according to the manufacturer's instructions. Then, 500 to 1,000 ng total RNA of the transfected cell cultures of pGECs and pGFs was sequenced with 16 million reads (75-bp single end) on a NextSeq 500 using the NextSeq 500/550 High Output Kit v2.5 (75 cycles). RNA-Seq was performed at the Berlin Institute of Health Core Facility Genomics. Reads were aligned to the Genome Reference Consortium Human Build 38 patch release 7 (GRCh38.p7) genome using the STAR aligner v. 2.7.5a (Dobin et al. 2013). Quality control (QC) of the reads was inspected using the multiqc reporting tool (Ewels et al. 2016) summarizing a number of approaches, including fastqc (available online at <http://www.bioinformatics.babraham.ac.uk/projects/fastqc>), dupradar (Sayols et al. 2016), qualimap (Garcia-Alcalde et al. 2012), and RNA-SeqC (DeLuca et al. 2012). Raw counts were extracted using the STAR program. For differential gene expression, the R package DESeq2 (Love et al. 2014), version 1.26 was used. Gene set enrichment was performed using the CERNO test from the tmod package (Zyla et al. 2019), version 0.46.2 using the gene expression profiling-based gene set included in the package as well as the MSigDB (Liberzon et al. 2015). For the hypergeometric test and the Gene Ontology gene sets, the goseq package, version 1.38 (Young et al. 2010) was used. The *P* values of the differently expressed genes were corrected for multiple testing using Benjamini-Hochberg correction. The corrected *P* values are given as *q* values (false discovery rate [FDR]).

Scanning Electron Microscopy

The samples were fixed in glutaraldehyde, washed in H₂O, and dehydrated in ethanol (15%–100%). Drying was done in a Polaron Critical-Point Dryer. Palladium coating for electric conductivity was performed with a Polaron E 5100 sputter coater. Electron microscopy was completed with a FEI Quanta 250 field emission scanning electron microscope. Images of secondary and backscattered electron images were mixed in Photoshop (Adobe).

Results

Direct contact of *E. gingivalis* to pGECs for 2 h increased the expression of a variety of multifunctional proinflammatory

cytokine and chemokine genes. The most upregulated genes were tumor necrosis factor α (*TNF*) with a fold change (FC) of 430 and interleukin 8 (*IL8*, FC = 359), followed by C-C motif chemokine ligand 20 (*CCL20*, FC = 169), C-X-C motif chemokine ligand 2 (*CXCL2*, FC = 160), and colony stimulating factor 1 (*CSF1*, FC = 100; Table).

Direct contact of *E. gingivalis* to pGFs increased the expression of a variety of genes that were distinct to those differentially expressed in pGECs. Furthermore, the increase in gene expression was explicitly lower compared to the response in pGECs. The genes that showed most increased expression with $P < 5 \times 10^{-16}$ were the transcriptional regulators zinc finger protein 331 (*ZNF331*, FC = 18), nuclear receptor subfamily 4 group A member 3 (*NR4A3*, FC 15), and the proinflammatory cytokine interleukin-11 (*IL-11*, FC 11; Table).

Gene set enrichment analysis using a second-generation algorithm contrasting *E. gingivalis*-infected pGECs compared to uninfected pGECs as controls showed the highest effect sizes (ESs) for the gene set “chemokines and inflammatory molecules in myeloid cells” (LI.M86.0) with an area under the curve (AUC) = 0.90 (ES = 5.15, adjusted $P = 3.1 \times 10^{-19}$), “signaling in T cells” (LI.M35.0) with an AUC = 0.97 (ES = 5.16, adjusted $P = 6.0 \times 10^{-9}$), and “cell cycle and growth arrest” (LI.M31) with AUC = 0.94 (ES = 5.03, adjusted $P = 2 \times 10^{-10}$) (Fig. 1, Appendix Table 1).

E. gingivalis-infected pGFs showed the highest AUC and ES for the gene set “cell cycle and growth arrest” (LI.M31) with AUC = 0.91 (ES = 4.56, adjusted $P = 4.8 \times 10^{-9}$), followed by the gene sets “putative targets of PAX3” (LI.M89) with AUC = 0.90 (ES = 3.95, adjusted $P = 2.8 \times 10^{-10}$), “chemokines and inflammatory molecules in myeloid cells” (LI.M86.0) with AUC = 0.86 (ES = 4.43, adjusted $P = 3.5 \times 10^{-15}$), and “signaling in T cells” (LI.M35.0) with an AUC = 0.88 (ES = 4.08, adjusted $P = 4.0 \times 10^{-6}$; Fig. 1, Appendix Table 1). Furthermore, the gene set enrichment analysis showed that *E. gingivalis* infection of pGFs but not of pGECs correlated with significant downregulation of several gene sets related to cell cycle regulation (Fig. 2). The top 2 most downregulated gene sets in pGFs were cell cycle (DC.M3.3) with AUC = 0.84 (ES = 2.27, adjusted $P = 3.3 \times 10^{-9}$) and “PLK1 signaling events” (LI.M4.2) with AUC = 0.85 (ES = 2.37, adjusted $P = 1.95 \times 10^{-7}$; Appendix Table 1).

To identify microRNAs (miRNAs) that are affected by *E. gingivalis* infection, we also performed a tmod enrichment analysis for database microRNA targets from the Molecular Signatures DB (MSigDB). In *E. gingivalis*-stimulated pGECs and pGFs, the gene set enrichment analysis identified 6 and 2 gene sets, respectively, which were listed in MSigDB as regulated by a specific miRNA. These miRNAs and the genes of these gene sets that were differentially expressed in our experiments are listed in Appendix Table 2.

Scanning electron microscopy showed distinct behavior patterns of *E. gingivalis* on the gingival epithelial monolayer (Fig. 3). We observed that it slid a pseudopodium under a gingival epithelial cell and attached to a gingival epithelial cell at the host cell's nucleus. It exhibited long cylindrical structures, termed *digipodia*, which made contact with the target cell,

Table. Differential Expressed Genes ($\log_2FC > 3$) in *Entamoeba gingivalis*-Infected Gingival Epithelial and Fibroblast Cells.

Gene Name	BaseMean	Log ₂ FoldChange	LFCSE	Fold Change
pGECs				
<i>TNF</i>	1,377.89	8.74	0.22	429.57
<i>IL8</i>	22,941.70	8.48	0.12	359.05
<i>CCL20</i>	932.68	7.38	0.19	168.57
<i>CXCL2</i>	4,522.85	7.30	0.14	159.59
<i>CSF2</i>	745.08	6.62	0.17	100.36
<i>CXCL1</i>	8,045.37	5.94	0.09	63.39
<i>CSF3</i>	680.52	5.42	0.13	44.81
<i>TNFAIP3</i>	31,885.55	5.26	0.06	40.32
<i>NFKBIZ</i>	9,296.60	5.11	0.07	36.54
<i>INHBA</i>	4,286.42	4.57	0.06	25.75
<i>NFKBIA</i>	9,981.93	4.55	0.05	25.43
<i>HBEGF</i>	3,306.39	4.45	0.06	23.86
<i>PRDM1</i>	1,391.96	4.42	0.09	23.41
<i>DUSP1</i>	9,213.66	4.37	0.07	22.68
<i>SOC3</i>	2,556.20	4.34	0.11	22.25
<i>IL1A</i>	8,885.05	4.25	0.06	21.03
<i>PNRC1</i>	2,230.03	3.98	0.10	17.78
<i>PPP1R15A</i>	8,594.85	3.93	0.07	17.24
<i>IER3</i>	16,231.18	3.76	0.05	15.55
<i>EGR1</i>	10,059.92	3.71	0.10	15.09
<i>EFNA1</i>	1,794.90	3.65	0.07	14.55
<i>IL1B</i>	10,123.23	3.24	0.04	11.45
<i>IL36G</i>	735.94	3.14	0.07	10.82
pGFs				
<i>ZNF331</i>	3,445.26	4.00	0.08	18.00
<i>NR4A3</i>	9,317.48	3.66	0.08	14.64
<i>IL11</i>	1,894.79	3.12	0.08	10.69
<i>CHMP1B</i>	2,168.48	3.00	0.06	10.00
<i>BTG2</i>	2,212.23	2.96	0.07	9.78
<i>ACKR3</i>	1,088.72	2.89	0.07	9.41
<i>ATF3</i>	4,080.01	2.58	0.07	7.98
<i>SLC2A3</i>	2,589.91	2.00	0.05	6.00
<i>SGK1</i>	7,787.43	2.15	0.06	6.44
<i>FOS</i>	1,632.41	3.20	0.09	11.19
<i>GPCPD1</i>	1,325.49	2.11	0.06	6.32

Differentially expressed genes are shown with \log_2 foldchange >3 for pGECs and \log_2 foldchange >2 for pGFs. All genes showed significant differential expression with P values $< 5 \times 10^{-16}$.

LFCSE, logfold change standard error; pGEC, primary gingival epithelial cell; pGF, primary gingival fibroblast.

extending into the cytoplasm, possibly extending into the nucleus. We also observed that *E. gingivalis* seemed to penetrate the host cells not randomly but chose those areas of the cells where the nuclei locate. In addition, we observed that *E. gingivalis* made contact with target cells by exhibiting long cylindrical structures, termed *digipodia*. Furthermore, the protozoan moved on the epithelial cell barrier and accumulated in interstices of the culture plates (Appendix Fig. 1).

Discussion

Approximately 15% of the healthy oral cavities of adults are infected with *E. gingivalis*. The prevalence of this protozoan strongly increases in periodontal inflammation, and it colonizes up to 80% of inflamed pockets of patients with periodontitis. Colonization can be asymptomatic, and the established

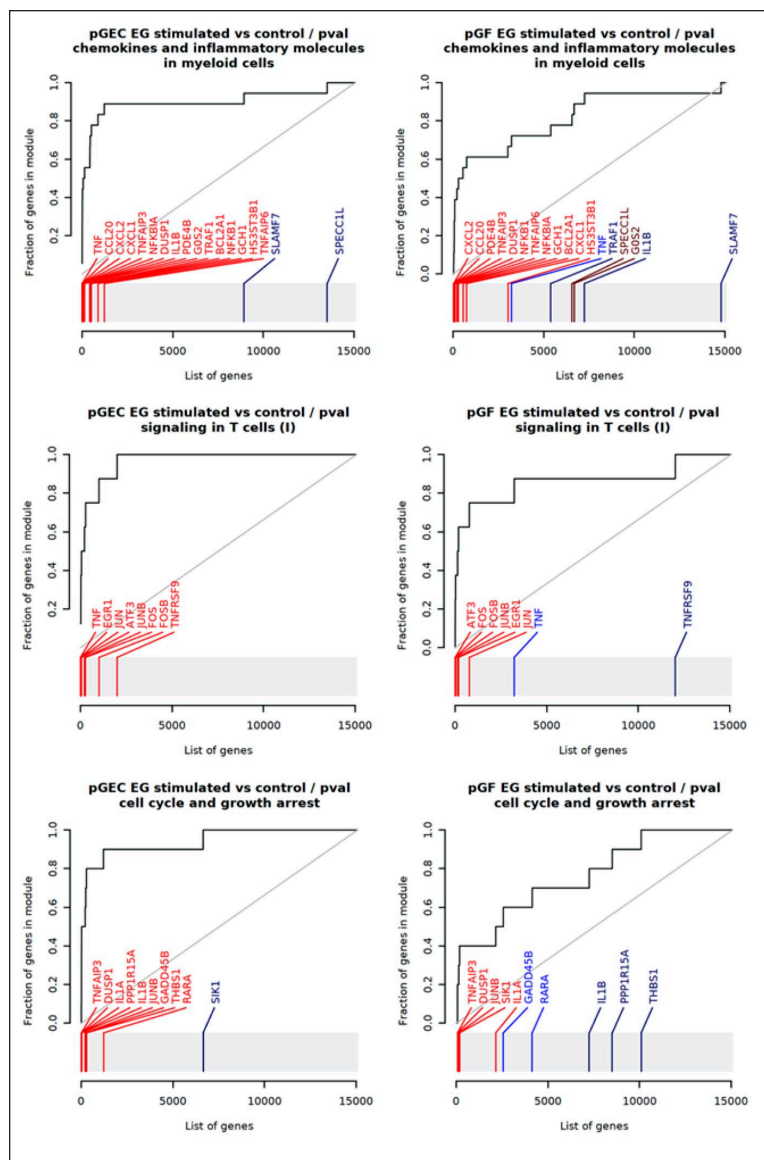


Figure 1. Evidence plots for the top 3 gene sets in the enrichment test *Entamoeba gingivalis*-infected versus mock-infected primary gingival epithelial cells (pGECs) and primary gingival fibroblasts (pGFs). Figures show the evidence plots for the top 3 gene sets with the existing evidence for the enrichment of the given gene set in the given contrast. Each row corresponds to 1 gene set. The left column corresponds to the enrichment tests pGECs + *E. gingivalis* versus pGECs + mock infection. The right column corresponds to the enrichment tests pGFs + *E. gingivalis* versus pGFs + mock infection. The curve shows the receiver operator characteristic (ROC) curve for a given gene set. The scale below the figure represents the ordered list of genes. Genes belonging to a given gene set are highlighted. Colors indicate whether the genes are positively or negatively regulated (red or blue, respectively), while color brightness indicates whether genes are significantly regulated (at $q < .05$).

paradigm has been that it does not cause or contribute to periodontal tissue destruction and increased inflammation. In the current study, we showed that direct cell contact of *E. gingivalis* to gingival epithelial cells induced a very strong innate immune response with the cytokines *TNF* and *IL8*, showing a 430- and 360-fold increase of expression, respectively. *IL8* is

the main neutrophil chemotactic factor, inducing chemotaxis and phagocytosis of neutrophils in target cells. However, neutrophils seem to have little effect on *E. gingivalis* and were observed to be target cells of amoebic phagocytosis (Bonner et al. 2018). *TNF* is involved in the regulation of a wide spectrum of biological processes, including proinflammatory mechanisms, for example, by stimulation of interleukin-1 secretion and apoptosis. There is also evidence that *TNF* has a role in epithelial barrier dysfunction by increasing tight junction permeability (Mullin et al. 1992) and apoptosis of human epithelial cells (Gitter et al. 2000). The function of *TNF*- α to induce leaks in the epithelial barrier, together with the strong activation of *TNF* expression in gingival epithelial cells following infection with *E. gingivalis*, may help this parasite to disrupt epithelial barrier function. Providing further evidence of the proinflammatory potential of *E. gingivalis* is the strong activation of other genes involved in immunoregulatory and inflammatory processes such as the chemokines *CCL20* (170-fold) and *CXCL2* (160-fold). In contrast to gingival epithelial cells, where *E. gingivalis* strongly activated genes that regulate inflammatory responses of the innate immune system by the factor of several hundreds, in gingival fibroblasts, the effect of *E. gingivalis* on gene expression was less strong and influenced genes with different functions. For example, the top 2 upregulated genes, *ZNF331* (18-fold) and *NR4A3* (15-fold), are considered tumor suppressors (Jiang et al. 2015; Shimizu et al. 2016; Yeh et al. 2016; Wang et al. 2017) and play roles in the regulation of cell proliferation. Top 3 upregulated gene *IL11* (11 fold) is expressed specifically in fibroblasts, in which it drives ERK-dependent autocrine signaling that is required for fibrogenic protein synthesis (Schafer et al. 2017). Different cell type effects of *E. gingivalis* on epithelial cells and fibroblasts were also implied by the gene set enrichment analyses. In pGFs, the gene sets “cell cycle and growth arrest” and “putative targets of PAX3” showed the highest AUCs, followed by the gene set “signaling in T cells,” whereas in pGECs, the gene sets “signaling in T cells” and “chemokines and inflammatory molecules in myeloid cells” showed the highest AUC, followed by the gene sets “cell cycle and growth arrest.” Moreover, the strong downregulation of the gene sets “cell cycle” and “PLK1 signaling events” in pGFs, which was not observed in pGECs, indicated that in pGFs, *E. gingivalis* essentially induced inhibition of cell proliferation and apoptosis. We note that we also found gene enrichment for miRNA targets from the Molecular Signatures DB (MSigDB) for contrast *E. gingivalis*-stimulated pGECs

and pGFs versus controls (Appendix). There is some evidence that the microbiota affects host health by regulating host miRNAs (Nguyen et al. 2014; Yu et al. 2017). How the microbiota regulates miRNAs is still unknown, but microbial metabolites may regulate miRNA functions (Dalmasso et al. 2014). Future studies may aim to identify miRNA and their target genes that are differentially regulated by specific microorganisms and explore the mechanism by which oral microorganisms influence the expression of these miRNAs.

We observed different behavior patterns of *E. gingivalis* on the gingival epithelial layer. We showed that it aimed to slide its pseudopodium under a gingival epithelial cell and that it accumulated in interstices of the culture plates. This may illustrate colonization behavior seeking for grooves. We also showed that it attaches to gingival epithelial cells at the location of the host cell's nucleus. Here, it exhibited digipodia, which made contacts with the target cell, extending into the cytoplasm, possibly protruding into the nucleus. This observation argues that *E. gingivalis*, similar to other parasitic protozoa, uses a process termed *trogocytosis* to ingest material from the target cell. It is also possible that *E. gingivalis* also secretes material into the target cells to induce apoptosis or necrosis. For example, it was previously shown for the protozoan *Acanthamoeba* that cells targeted by digipodia eventually died (Pettit et al. 1996; Rocha-Azevedo et al. 2006). The strong upregulation of TNF following *E. gingivalis* stimulation may further promote leaks in the epithelial barrier caused by TNF- α -induced tight junction permeability, thus increasing barrier impairment.

In conclusion, we showed that *E. gingivalis* overcomes the epithelial barrier through killing the cells by trogocytosis, probably ingesting their nuclei. Following infection of the epithelial barrier monolayer, the parasite also induces a very strong innate immune response in these cells, particularly characterized by strong expression of *TNF*, *IL8*, and proinflammatory chemokines. This may further contribute to impaired barrier integrity. Gingival fibroblasts show a different response, particularly characterized by inhibition of cell proliferation and induction of proapoptotic pathways. Our data imply that *E. gingivalis* has strong potential to cause and promote inflammation and to actively invade the oral mucosa, where it may contribute to profound tissue destruction. In addition, it likely aids other microorganisms to invade the oral mucosa, where they may further enter into the circulation with potential damaging effects on the vasculature. What drives host cell-killing activity of the amoebae in vivo and, if long-lasting, elimination of *E. gingivalis* from the inflamed periodontal

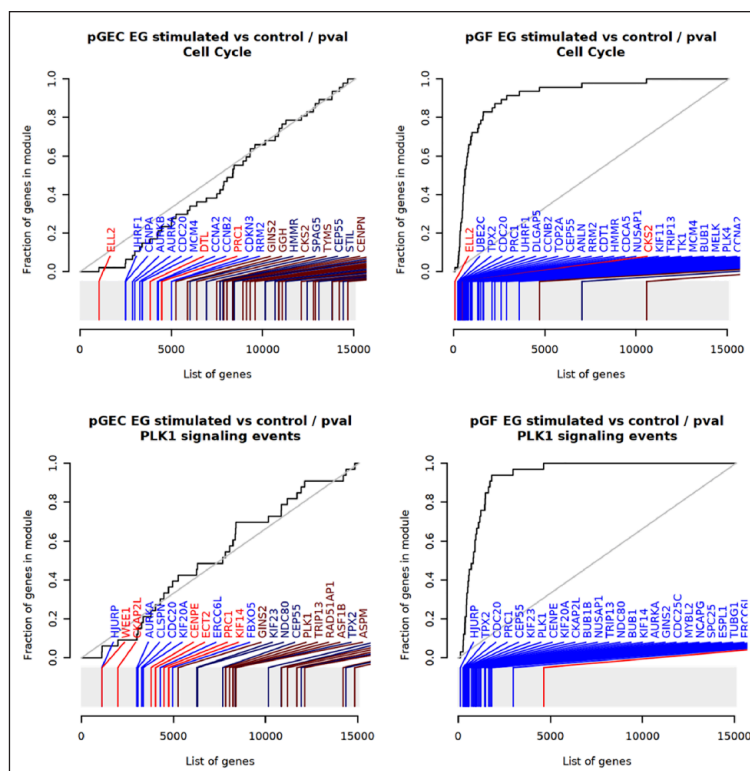


Figure 2. Evidence plots for the top 2 downregulated gene sets in primary gingival fibroblasts after *Entamoeba gingivalis* infection.

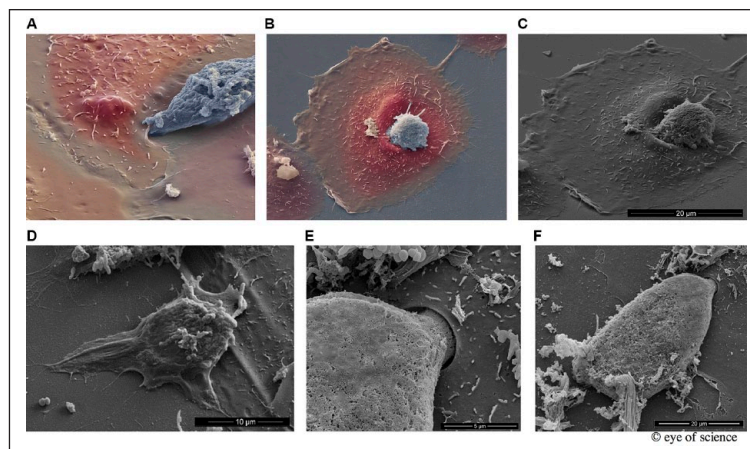


Figure 3. Behavior patterns of *Entamoeba gingivalis* on the gingival epithelial monolayer. Clockwise from left: (A) *E. gingivalis* slides a pseudopodium under a gingival epithelial cell. The elevation left of the amoeba indicates the position of the host cell's nucleus. (B) The amoeba is attached to a gingival epithelial cell at the host cell's nucleus. It exhibits long cylindrical structures, termed *digipodia*, that made contact with the target cell. (C) The same amoeba as in panel B from a different perspective. (D) *E. gingivalis* moves from a gingival cell (right) onto the surface of the culture plate, forming several flat pseudopods (possibly in the search for another cell). Parallel to the formation of the pseudopods, the amoeba's body has flattened, revealing a specific circular disk. (E) A digipodium is extending from *E. gingivalis* into the gingival epithelial cell. The pore in the host cell's membrane shows clean-cut edges. The digipodia appears to be in the process of secreting material into the target cell or ingesting material from the target cell in a process termed *trogocytosis*. The elevation of the host cell close to the opening suggests that the digipodia extended into the nucleus of the cell as previously illustrated by us using light microscopy (Bao et al. 2020). (F) General view of the same amoeba as in panel E.

pockets by an antiparasitic therapy might have potential to arrest and resolve oral inflammation and to improve periodontal healing.

Author Contributions

X. Bao, contributed to conception, design, data acquisition, and analysis, drafted and critically revised the manuscript; J. Weiner 3rd, contributed to data analysis, critically revised the manuscript; O. Meckes, H. Dommisch, contributed to data acquisition, critically revised the manuscript; A. Schaefer, contributed to conception, design, data acquisition, and interpretation, drafted and critically revised the manuscript. All authors gave final approval and agree to be accountable for all aspects of the work.

Acknowledgments

We thank Jim Rheinwald (Boston, MA) for providing us with the cell line OKG4/bmi1/TERT.

Declaration of Conflicting Interests


The authors declared no potential conflicts of interest with respect to the research, authorship, and/or publication of this article.

Funding

The authors disclosed receipt of the following financial support for the research, authorship, and/or publication of this article: This work was funded by the German Research Foundation (Deutsche Forschungsgemeinschaft DFG) to AS (SCHA1582-7-1) and by the Chinese Scholarship Council, China.

ORCID iDs

X. Bao  <https://orcid.org/0000-0003-0262-1719>

H. Dommisch  <https://orcid.org/0000-0003-1043-2651>

References

- Bao X, Wiehe R, Dommisch H, Schaefer AS. 2020. *Entamoeba gingivalis* causes oral inflammation and tissue destruction. *J Dent Res*. 99(5):561–567.
- Bonner M, Amard V, Bar-Pinatel C, Charpentier F, Chatard JM, Desmuyck Y, Ihler S, Rochet JP, Roux de La Tribouille V, Saladin L, et al. 2014. Detection of the amoeba *Entamoeba gingivalis* in periodontal pockets. *Parasite*. 21:30.
- Bonner M, Fresno M, Girones N, Guillen N, Santi-Rocca J. 2018. Reassessing the role of *Entamoeba gingivalis* in periodontitis. *Front Cell Infect Microbiol*. 8:379.
- Dalmasso G, Coughnoux A, Delmas J, Darfeuille-Michaud A, Bonnet R. 2014. The bacterial genotoxin colibactin promotes colon tumor growth by modifying the tumor microenvironment. *Gut Microbes*. 5(5):675–680.
- DeLuca DS, Levin JZ, Sivachenko A, Fennell T, Nazaire MD, Williams C, Reich M, Winckler W, Getz G. 2012. RNA-SeQC: RNA-seq metrics for quality control and process optimization. *Bioinformatics*. 28(11):1530–1532.
- Deng ZL, Szafranski SP, Jarek M, Bhuju S, Wagner-Dobler I. 2017. Dysbiosis in chronic periodontitis: key microbial players and interactions with the human host. *Sci Rep*. 7(1):3703.
- Dickson MA, Hahn WC, Ino Y, Ronfard V, Wu JY, Weinberg RA, Louis DN, Li FP, Rheinwald JG. 2000. Human keratinocytes that express hTERT and also bypass a p16(INK4a)-enforced mechanism that limits life span become immortal yet retain normal growth and differentiation characteristics. *Mol Cell Biol*. 20(4):1436–1447.
- Dobin A, Davis CA, Schlesinger F, Drenkow J, Zaleski C, Jha S, Batut P, Chaisson M, Gingeras TR. 2013. STAR: ultrafast universal RNA-seq aligner. *Bioinformatics*. 29(1):15–21.
- Ewels P, Magnusson M, Lundin S, Kaller M. 2016. MultiQC: summarize analysis results for multiple tools and samples in a single report. *Bioinformatics*. 32(19):3047–3048.
- Garcia-Alcalde F, Okonechnikov K, Carbonell J, Cruz LM, Gotz S, Tarazona S, Dopazo J, Meyer TF, Conesa A. 2012. Qualimap: evaluating next-generation sequencing alignment data. *Bioinformatics*. 28(20):2678–2679.
- Gitter AH, Bendfeldt K, Schulzke JD, Fromm M. 2000. Leaks in the epithelial barrier caused by spontaneous and TNF-alpha-induced single-cell apoptosis. *FASEB J*. 14(12):1749–1753.
- Jiang S, Linghu E, Zhan Q, Han W, Guo M. 2015. Methylation of znf331 promotes cell invasion and migration in human esophageal cancer. *Curr Protein Pept Sci*. 16(4):322–328.
- Liberzon A, Birger C, Thorvaldsdottir H, Ghandi M, Mesirov JP, Tamayo P. 2015. The Molecular Signatures Database (MSigDB) hallmark gene set collection. *Cell Syst*. 1(6):417–425.
- Love MI, Huber W, Anders S. 2014. Moderated estimation of fold change and dispersion for RNA-seq data with DESeq2. *Genome Biol*. 15(12):550.
- Lyons T, Stanfield E. 1989. Introduction to protozoa and fungi in periodontal infections: a manual of microbiological diagnosis and nonsurgical treatment. Ottawa: Trevor Lyons.
- Mullin JM, Laughlin KV, Marano CW, Russo LM, Soler AP. 1992. Modulation of tumor necrosis factor-induced increase in renal (LLC-PK1) transepithelial permeability. *Am J Physiol*. 263:F915–F924.
- Nguyen HT, Dalmasso G, Muller S, Carriere J, Seibold F, Darfeuille-Michaud A. 2014. Crohn's disease-associated adherent invasive *Escherichia coli* modulate levels of microRNAs in intestinal epithelial cells to reduce autophagy. *Gastroenterology*. 146(2):508–519.
- Pettit DA, Williamson J, Cabral GA, Marciano-Cabral F. 1996. In vitro destruction of nerve cell cultures by *Acanthamoeba* spp.: a transmission and scanning electron microscopy study. *J Parasitol*. 82(5):769–777.
- Ralston KS, Petri WA Jr. 2011. Tissue destruction and invasion by *Entamoeba histolytica*. *Trends Parasitol*. 27(6):254–263.
- Ralston KS, Solga MD, Mackey-Lawrence NM, Somlata, Bhattacharya A, Petri WA Jr. 2014. Trophocytosis by *Entamoeba histolytica* contributes to cell killing and tissue invasion. *Nature*. 508(7497):526–530.
- Rocha-Azevedo B, Menezes GC, Silva-Filho FC. 2006. The interaction between *Acanthamoeba polyphaga* and human osteoblastic cells in vitro. *Microb Pathog*. 40(1):8–14.
- Rosenbaum J, Usyk M, Chen Z, Zolnik CP, Jones HE, Waldron L, Dowd JB, Thorpe LE, Burk RD. 2019. Evaluation of oral cavity DNA extraction methods on bacterial and fungal microbiota. *Sci Rep*. 9(1):1531.
- Sayols S, Scherzinger D, Klein H. 2016. dupRadar: a Bioconductor package for the assessment of PCR artifacts in RNA-Seq data. *BMC Bioinformatics*. 17(1):428.
- Schafer S, Viswanathan S, Widjaja AA, Lim WW, Moreno-Moral A, DeLaughter DM, Ng B, Patone G, Chow K, Khin E, et al. 2017. IL-11 is a crucial determinant of cardiovascular fibrosis. *Nature*. 552(7683):110–115.
- Shimizu R, Muto T, Aoyama K, Choi K, Takeuchi M, Koide S, Hasegawa N, Isshiki Y, Togasaki E, Kawajiri-Manako C, et al. 2016. Possible role of intragenic DNA hypermethylation in gene silencing of the tumor suppressor gene NR4A3 in acute myeloid leukemia. *Leuk Res*. 50:85–94.
- Trim RD, Skinner MA, Farone MB, Dubois JD, Newsome AL. 2011. Use of PCR to detect *Entamoeba gingivalis* in diseased gingival pockets and demonstrate its absence in healthy gingival sites. *Parasitol Res*. 109(3):857–864.
- Wang Y, He T, Herman JG, Linghu E, Yang Y, Fuks F, Zhou F, Song L, Guo M. 2017. Methylation of ZNF331 is an independent prognostic marker of colorectal cancer and promotes colorectal cancer growth. *Clin Epigenetics*. 9:115.
- Yeh CM, Chang LY, Lin SH, Chou JL, Hsieh HY, Zeng LH, Chuang SY, Wang HW, Dittmer C, Lin CY, et al. 2016. Epigenetic silencing of the NR4A3 tumor suppressor, by aberrant JAK/STAT signaling, predicts prognosis in gastric cancer. *Sci Rep*. 6:31690.
- Young MD, Wakefield MJ, Smyth GK, Oshlack A. 2010. Gene ontology analysis for RNA-seq: accounting for selection bias. *Genome Biol*. 11(2):R14.
- Yu T, Guo F, Yu Y, Sun T, Ma D, Han J, Qian Y, Kryczek I, Sun D, Nagarsheth N, et al. 2017. *Fusobacterium nucleatum* promotes chemoresistance to colorectal cancer by modulating autophagy. *Cell*. 170(3):548–563.e16.
- Zyla J, Marczyk M, Domaszewska T, Kaufmann SHE, Polanska J, Weiner J. 2019. Gene set enrichment for reproducible science: comparison of CERNO and eight other algorithms. *Bioinformatics*. 35(24):5146–5154.